frontiers | Frontiers in Materials

TYPE Original Research
PUBLISHED 09 May 2025
DOI 10.3389/fmats.2025.1579229

OPEN ACCESS

EDITED BY
Antonios Kanellopoulos,
University of Hertfordshire, United Kingdom

REVIEWED BY
Chuanqing Fu,
Zhejiang University of Technology, China
Yingbin Wang,
Hubei University of Technology, China
Qiang Fu,
Xi'an University of Architecture and Technology, China
Peng Du,
University of Jinan, China

*CORRESPONDENCE
Songfu Yuan,
2310474031@email.szu.edu.cn

RECEIVED 18 February 2025
ACCEPTED 23 April 2025
PUBLISHED 09 May 2025

CITATION
Tan H, Feng B, Liu Y, Zhou J, Liu J and Yuan S (2025) Disposal and application of discarded nitrile gloves in sustainable cement-based materials.
Front. Mater. 12:1579229.
doi: 10.3389/fmats.2025.1579229

Disposal and application of discarded nitrile gloves in sustainable cement-based materials

Haoyu Tan[1], Baoping Feng[1], Yige Liu[2], Junyi Zhou[3], Junyao Liu[3] and Songfu Yuan[3]*

[1]CCCC-SHEC Dongmeng Engineering Co., Ltd., Xi'an, China, [2]Shenzhen No. 2 Experimental School, Shenzhen, China, [3]Guangdong Provincial Key Laboratory of Durability for Marine Civil Engineering, College of Civil and Transportation Engineering, Shenzhen University, Shenzhen, China

This study focuses on the application of shredded waste nitrile glove fibers (SWNGF) in sustainable cement-based materials, aiming to address the challenges of personal protective equipment (PPE) waste disposal and explore new uses in the construction sector. Specimens were prepared using Conch brand ordinary Portland cement as the base material, mixed with pure water, and incorporated with varying volumes (0%, 1%, 2%, and 3%) and sizes (15 mm × 5 mm, 20 mm × 5 mm, 15 mm × 10 mm) of SWNGF. Through compressive strength, flexural strength tests, and SEM analysis, the results revealed that both compressive and flexural strengths decreased with increasing SWNGF content, with the 15 mm × 10 mm size showing relatively better performance in terms of both compressive and flexural strength. Compressive strain initially increased and then decreased, with the 20 mm × 5 mm size favoring compressive strain. Flexural deflection increased steadily for Group A, followed by an initial increase and then a decrease for Group B, while Group C showed a consistent rise. Incorporating SWNGF improved flexural toughness, with post-failure results showing that specimens C3 at T_{d3} and T_{d5}, and A3 at T_{d5} and T_{d10} performed better. Microscopically, the bond between the gloves and the cement matrix showed gaps, but the flexibility of the rubber improved performance. The surface characteristics of SWNGF facilitated bonding, and multiple hydration products were observed in the cement matrix, with some interconnected pores affecting the density. This study provides data support and theoretical basis for the application of SWNGF in concrete, holding significant potential for promoting the sustainable use of waste PPE in the construction industry.

KEYWORDS

shredded waste nitrile glove fibers, fiber reinforced cement composites, compressive strength, flexural strength, microstructure

1 Introduction

Since the outbreak of the COVID-19 pandemic, the global influenza outbreak triggered by the virus has had widespread and profound impacts on numerous countries and regions. It has not only posed a significant threat to human health but also placed unprecedented pressure on the economies, social order, and public health systems of

various nations. In response, many nations have implemented regulations requiring the use of PPE), including masks, gloves, face shields, protective clothing, and aprons. These protective gear are essential for safeguarding individuals from pathogens and contaminants (Anastopoulos and Pashalidis, 2021; Boroujeni et al., 2021; Chua et al., 2020), resulting in a significant increase in the usage of PPE (MDS, 2023). The disposal of medical waste after use is a lengthy process (Karimi et al., 2024; Park, 2023; Tang et al., 2023; Cao et al., 2023a; Cao et al., 2023b). The remaining large amounts of medical waste include disposable protective items such as masks (Idowu and Olonimoyo, 2023; Sangkham, 2020), gloves (Ran et al., 2023; Kilmartin-Lynch et al., 2022), protective clothing (Ran et al., 2022; Zeng et al., 2024), syringes and other medical instruments and devices (Karimi et al., 2024), catheters (Ramalingam et al., 2023), needles (Demir and Moslem, 2024), pharmaceutical packaging (Masud et al., 2023), waste containers for medical waste and waste liquids, medical waste bags and packaging (Dadwal et al., 2023), as well as infectious waste (Chowdhury et al., 2022). Nitrile gloves, which are widely utilized not only in medical practices but also in sectors such as sanitation, personal care, food processing, beverage production, pharmaceuticals, chemical manufacturing, automotive industry, electronics manufacturing, construction, and research laboratories, are in high demand (Telugunta et al., 2021). By 2027, the global demand for nitrile gloves is projected to increase at an annual growth rate of 10.6%–11.2% (Patrawoot et al., 2021). However, the waste management strategies implemented by various countries for PPE are largely similar, predominantly relying on incineration and landfill disposal (Asim et al., 2021; Silva, 2021). Although incineration of plastic-based PPE waste effectively eliminates viruses, it also results in the release of substantial amounts of greenhouse gases and harmful substances, including dioxins, furans, and polychlorinated biphenyls (PCBs) (Zhu et al., 2022; Cheng et al., 2024). Consequently, finding sustainable solutions for the disposal of PPE waste has become a global challenge.

Despite the environmental challenges posed by PPE waste, the mechanical properties of its polymer materials can precisely compensate for the brittleness of cement-based materials. They demonstrate high corrosion resistance, capable of withstanding acid and alkali corrosion. These materials possess excellent durability and stability, ensuring long-term performance retention. Their high tensile strength provides reliable support for structural applications. Additionally, their low density makes them lightweight and easy to handle during construction. With minimal water absorption, they are unaffected by humid environments, making them an ideal choice for building materials (Zhu et al., 2022). In recent years, with the growing awareness of environmental sustainability, the management of plastic-based PPE waste has become a focal point. Items such as discarded masks, gloves, and protective clothing are being studied for their potential reuse in the construction sector. Researchers are exploring methods to repurpose plastic-based PPE waste materials for various building applications. Existing studies have shown that utilizing PPE waste to enhance the physical and stability properties of construction materials, such as subbases, base layers, roadbeds, bricks, concrete, and mortar, holds significant potential. For example, Zhu et al. (2022). Demonstrated that nitrile glove strips can serve as an additive to improve the reinforcement and stabilization of expansive clay subgrade surfaces. Compared to the soil control group without the addition of nitrile gloves, the incorporation of 1.5% nitrile glove waste resulted in a 24% increase in unconfined compressive strength, an 11% improvement in bearing capacity, a 41% enhancement in stiffness, and a 14% reduction in swelling-shrinkage potential. Kilmartin-Lynch et al. (2022). investigated the feasibility of incorporating plastic protective suits into concrete, finding that various performance parameters of the concrete were improved when shredded isolation suits were added, with the effects varying based on the volume content of the suits. Similarly, Saberian et al. (2021). Assessed the impact of disposable masks on road construction, concluding that adding 1%–2% of shredded masks to recycled concrete aggregates (RCA) enhanced the strength and stiffness of the concrete due to the reinforcing effect of the masks when combined with the RCA.

This study focuses on the effective incorporation of discarded nitrile gloves into concrete, using shredded waste nitrile gloves as a substitute for fiber reinforcement in cementitious composites. Freshwater was used as the mixing water, and four volume dosages (0%, 1%, 2%, and 3%) along with three different fiber sizes were tested. The mechanical properties of the cement-based materials were evaluated through compressive strength, flexural strength, and scanning electron microscopy (SEM) tests, analyzing the failure modes under compression and flexure. The study evaluated the compressive and flexural properties, focusing on load-bearing capacity, deformability, and energy absorption. The variations in mechanical performance were analyzed in relation to the microstructure and pore structure, and morphology of the materials. This research investigates how the size and dosage of nitrile glove fibers affect the mechanical properties of cement-based materials. By quantitatively analyzing the influence of these factors, valuable insights can be provided for optimizing the incorporation of nitrile glove waste.

2 Test design and raw materials

2.1 Raw materials

The cement used in this experiment was Conch brand ordinary Portland cement, produced in Yingde City, Guangdong Province, China, and conforms to the national standard GB 175-2023 (GB 175, 2023). The chemical composition of the cement was determined using an X-ray fluorescence spectrometer (XRF, model S4 PIONEER), with the specific data provided in Table 1. Figure 1 illustrates the dimensions and various parameters of the three sizes of shredded waste nitrile glove fibers (SWNGF) used in the experiment. The mixing water used was purified water that meets the requirements of JGJ63-2006 (JGJ 63, 2006).

2.2 Mix design

Table 2 presents the mix proportions used in this study. To investigate the effects of SWNGF on cement-based materials, SWNGF with a 0% volume content were used as a control group (CG). All groups were mixed with a water-to-cement ratio of 0.4 using pure water and ordinary Portland cement. The SWNGF was incorporated at volume percentages of 1%, 2%, and 3%, with

TABLE 1 Chemical content of cement.

%	CaO	SiO_2	Al_2O_3	Fe_2O_3	SO_3	MgO	K_2O
Cement	61.78	20.31	5.62	3.54	2.47	2.11	1.55

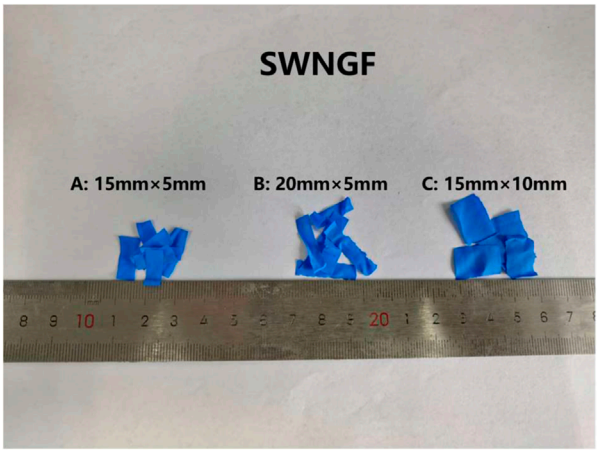

FIGURE 1
SWNGF **(A)** 15 mm × 5 mm. **(B)** 20 mm × 5 mm. **(C)** 15 mm × 10 mm.

TABLE 2 The proportion composition of each group of specimens.

Groups	Mixture NO.	w/b	Cement	SWNGF (Vol%)
CG		0.4	1	0
A	A-1	0.4	1	1
	A-2	0.4	1	2
	A-3	0.4	1	3
B	B-1	0.4	1	1
	B-2	0.4	1	2
	B-3	0.4	1	3
C	C-1	0.4	1	1
	C-2	0.4	1	2
	C-3	0.4	1	3

Note: w/b represents water-to-binder ratio.

specimen numbers designated as 1, 2, and 3, respectively. Three sizes of SWNGF fibers were selected (15 mm × 5 mm, 20 mm × 5 mm, and 15 mm × 10 mm), with specimen numbers represented as A, B, and C, respectively.

Specimens were prepared in accordance with GB/T 17671-1999 (GB/T 17671, 1999), with dimensions of 40 mm × 40 mm × 160 mm. The specimens were demolded after 24 h of rest and immediately placed in a constant temperature and humidity curing room for further curing. During the curing process, the temperature was precisely maintained within the range of 20°C ± 2°C, with a humidity level of over 95%. After 28 days of curing, the specimens were removed for subsequent testing.

2.3 Test method

2.3.1 Compressive and flexural test

The flexural and compressive strength tests were conducted following the guidelines outlined in the GB/T 17671-1999 standard (GB/T 17671, 1999). After a curing period of 28 days, the specimens were extracted from the curing environment and subsequently subjected to mechanical performance testing. The experiment was conducted using a constant load cement compressive and flexural testing machine (model YZH-300.10) manufactured by Zhejiang Luda Machinery Instrument Co, Ltd. At the start of the testing process, flexural tests were performed on the specimens, with the loading rate precisely controlled at 50 N/s. After completing the flexural tests, the fractured specimens were subjected to compressive tests, with the loading rate set at 2.5 kN/s.

According to ASTM C1018-97 (ASTM C 1018-97, 1998), the point where the first crack appears on the stress-strain curve is defined as the Limit of Proportionality (LOP), which marks the boundary between linear and nonlinear deformation of the material. The point corresponding to the peak stress after crack formation is referred to as the Modulus of Rupture (MOR), which reflects the maximum stress before material failure. In this study, the definitions of LOP and MOR are based on Zhang et al. (2022), and these two parameters were used as key indicators to evaluate both compressive and flexural performance. Through these parameters, the mechanical behavior of the material at the initial crack formation and at the maximum stress was analyzed, focusing on strength (load-bearing capacity), ductility (plastic deformation ability), and toughness (energy absorption capacity). Furthermore, LOP and MOR in the flexural test indicate the interaction between the fibers and the cement matrix.

As observed in Figure 2a, the compressive stress-strain curves of both the CG and SWNGF groups exhibit similar trends. Prior to reaching the LOP, the curves follow a linear progression. However, between LOP and the MOR, the slope of the curves gradually decreases, reaching zero at the MOR point. After reaching the MOR, the curve continues to decrease. As shown in Figure 2b, the flexural load-deflection curves of the CG and SWNGF groups also follow a linear development until reaching the LOP. Beyond the LOP, three distinct trends are typically observed. Ordinary cementitious materials are brittle, fracturing directly upon reaching the LOP. For fiber-reinforced engineered cementitious composites (ECCs), the specimens retain load-bearing capacity after fracture, displaying

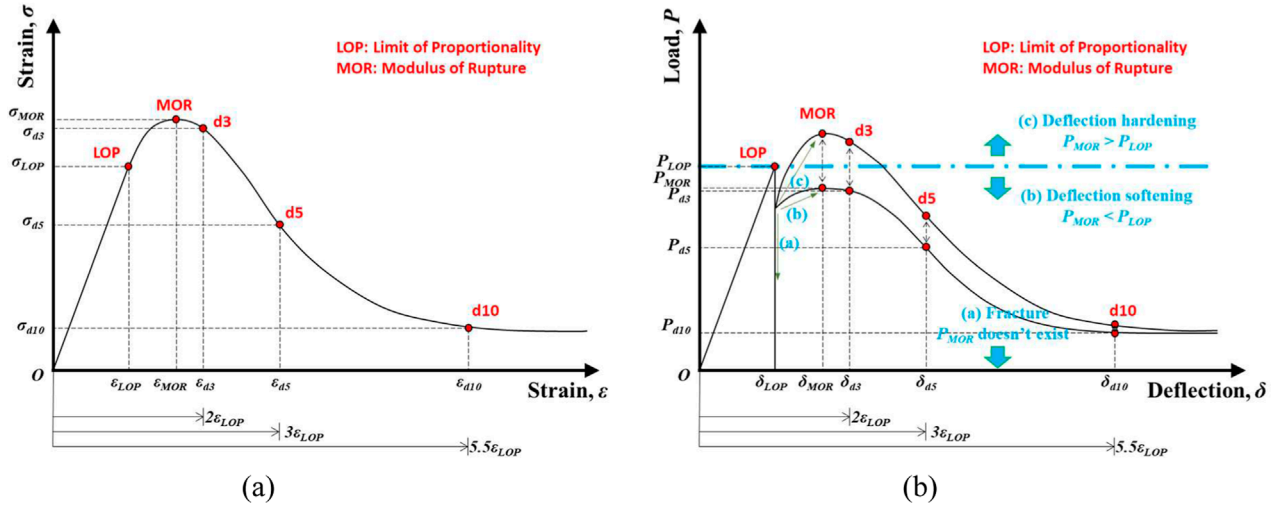

FIGURE 2
Mechanical response curve. **(a)** Compressive. **(b)** Flexural.

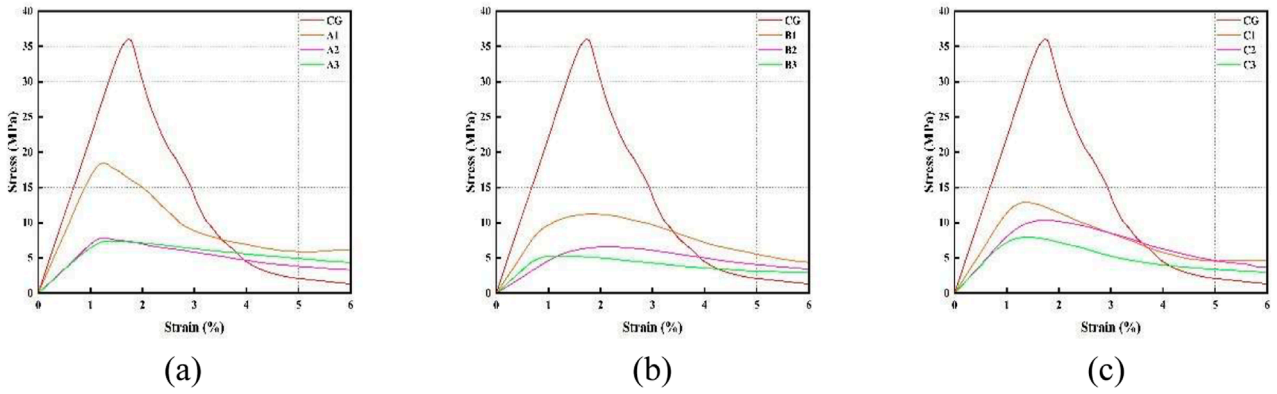

FIGURE 3
Compressive stress-strain curve. **(a)** Group A. **(b)** Group B. **(c)** Group C.

either deflection softening or deflection hardening behavior. In these cases, the load at the MOR point may be lower or higher than the load at the LOP. This phenomenon is primarily due to the role of the fibers in ECCs, which improve the toughness of the matrix, thereby enabling the specimens to retain a certain level of load-carrying capacity even after fracture initiation.

In the analysis of the compressive test results, a thorough evaluation was conducted for five key characteristic points (LOP, MOR, *d3*, *d5*, and *d10*) for all test samples. This encompasses the assessment and analysis of parameters such as load, stress, strain, and toughness. The analysis methodology was referenced from the literature (Zhang et al., 2022), and specific symbols were adopted to represent the parameters at each characteristic point: load is denoted as *P*, stress as σ, strain as ε, and toughness as *T*. For instance, In the analysis of the compressive stress-strain curve, specific symbols are used to represent key parameters associated with the MOR. Specifically, P_{MOR} denotes the load at the MOR, which can be directly obtained from the compressive stress-strain curve. σ_{MOR} is used to represent the compressive stress, which is derived from the measured load using the established calculation formula. Compressive strain ε is derived from displacement data, applying the relevant formula. Compressive toughness *T* is determined by calculating the area under the compressive stress-strain curve from the origin *O* to the MOR point. In this research, the material's energy absorption capacity under compression, compressive strength, and compressive deformation capacity are represented by T, σ, and ε, respectively.

When analyzing the results of the flexural strength test, a thorough evaluation of five key characteristic points (*d3*, *d5*, *d10*, MOR, and LOP) for all test samples is essential. This includes the measurement and analysis of parameters such as strength, load, toughness, and deflection. The analytical methods referenced in literature (Zhang et al., 2022) were followed, and specific symbols were adopted to represent the relevant parameters at each characteristic point: load is denoted as *P*, strength as *f*, deflection as δ, and toughness as *T*. For instance, In the curve

TABLE 3 Compressive characteristic parameters of CG and SWNGF.

Point	Proformance	Unit	CG	A-1	A-2	A-3	B-1	B-2	B-3	C-1	C-2	C-3
LOP	P_{LOP}	kN	48.62	19.44	10.04	9.27	14.52	10.67	7.95	20.75	13.88	10.81
	σ_{LOP}	MPa	30.39	12.15	6.28	5.79	9.07	6.67	4.97	12.97	8.68	6.76
	ε_{LOP}	%	1.55	1.02	1.51	1.07	1.04	1.66	1.01	1.26	1.21	1.20
	T_{LOP}	MPa	0.24	0.06	0.05	0.03	0.05	0.13	0.03	0.08	0.05	0.04
MOR	P_{MOR}	kN	52.22	23.45	12.02	10.64	16.62	11.91	9.48	22.59	14.85	11.71
	σ_{MOR}	MPa	32.63	14.65	7.51	6.65	10.39	7.45	5.93	14.12	9.28	7.32
	ε_{MOR}	%	1.77	1.46	2.29	1.80	1.59	2.40	1.92	1.60	1.67	1.67
	T_{MOR}	MPa	0.31	0.12	0.10	0.08	0.10	0.11	0.08	0.13	0.10	0.08
$d3$	T_{d3}	MPa	0.63	0.20	0.15	0.10	0.15	0.18	0.08	0.25	0.16	0.13
$d5$	T_{d5}	MPa	0.78	0.32	0.24	0.16	0.25	0.27	0.14	0.36	0.25	0.20
$d10$	T_{d10}	MPa	0.91	0.48	0.40	0.29	0.40	0.42	0.25	0.52	0.39	0.32

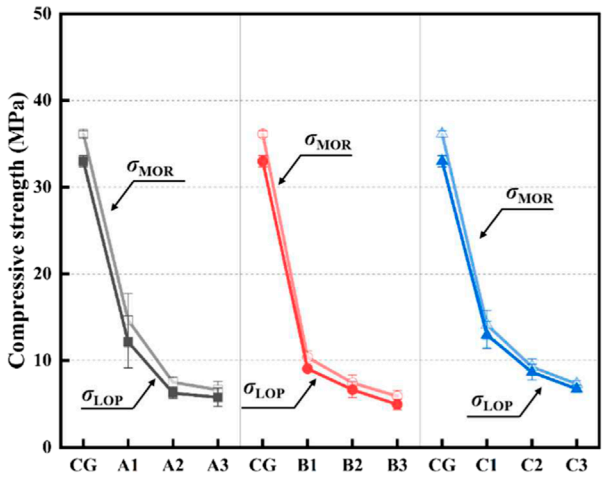

FIGURE 4
Compressive strength of CG and SWNGF.

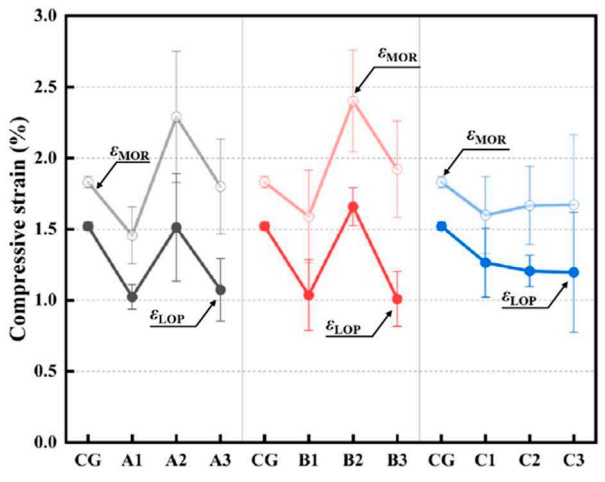

FIGURE 5
Compressive strain of CG and SWNGF.

depicting the relationship between flexural load and deflection, specific symbols are used to represent the key characteristics at the position corresponding to the MOR. Specifically, P_{MOR} denotes the load at this point, σ_{MOR} represents the strength, ε_{MOR} denotes the deflection, and T_{MOR} indicates the toughness. The load P and deflection ε are directly obtained from the flexural load-deflectiuation on curve, as for the flexural strength f, it is calculated using Equation 1. The flexural toughness T is determined by calculating the area under the flexural load-deflection curve from the origin O to the MOR point. In this research, the material's flexural strength, flexural deformation, and energy absorption capacity are represented by σ, ε, and T, respectively.

$$f = 1.5\frac{PS}{bh^2} \tag{1}$$

2.3.2 Scanning electron microscopy

After curing for 28 days, each group of samples was removed and immersed in isopropanol to prevent further hydration reactions. The samples were then placed in a vacuum drying oven at 50°C and dried to a constant weight. The microstructure of the samples was observed using a field emission scanning electron microscope (Quanta™ 250 FEG). Additionally, to obtain clearer

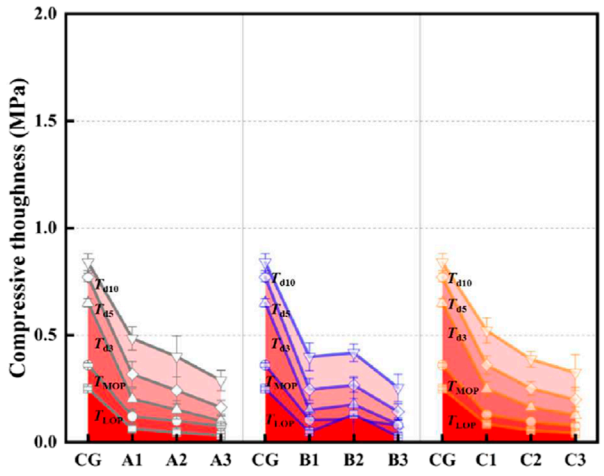

FIGURE 6
Compressive toughness of CG and SWNGF.

images, the samples were gold-coated prior to testing to enhance their conductivity.

3 Results and discussion

3.1 Mechanical properties under compression

3.1.1 The process of compressive failure

Figures 3a–c show the compressive stress-strain curves for groups A, B, and C. As seen in Figure 3, the compressive strength of groups A, B, and C decreases with increasing content of crushed nitrile gloves fibers, and a similar trend is observed for the elastic modulus. The compressive strength of the control group(CG) is 32.63 MPa, with A-1 exhibiting the highest compressive strength of all experimental groups at 14.65 MPa. However, there is some deviation in strain and toughness, and conclusions cannot be directly drawn from Figure 3.

Furthermore, as shown in Figure 3, both the compressive strength and the elastic modulus belonging to the CG are greater than those of the SWNGF groups. It is noteworthy that, upon specimen failure, the stress in the CG exhibits a rapid decline to a minimal value, whereas the stress in the SWNGF group decreases more gradually, ultimately surpassing that of the CG. Therefore, it can be concluded that while CG absorbs more energy before failure (reaching MOR), after specimen failure, SWNGF demonstrates superior energy absorption capability when the strain exceeds approximately 4%.

To further analyze the mechanical performance during the compressive process, the characteristic parameters of the compressive stress-strain curves for CG and SWNGF are summarized in Table 3, with each data point representing the average of six specimens.

3.1.2 Compressive strength

Figure 4 illustrates the compressive strength of CG and SWNGF, with the detailed data provided in Table 3. This section primarily discusses the two types of strength when the specimens reach LOP and MOR. As observed from Figure 4, the σ_{LOP} and σ_{MOR} of the CG group are 30.39 MPa and 32.63 MPa, respectively. The σ_{LOP} and σ_{MOR} of the SWNGF groups are all lower than those of the corresponding CG group. In group A, the σ_{LOP} and σ_{MOR} decreased to 5.79 MPa and 6.65 MPa, respectively; in group B, they decreased to 4.97 MPa and 5.93 MPa; and in group C, they decreased to 6.76 MPa and 7.32 MPa. This indicates that a high content of waste nitrile glove fibers is detrimental to the compressive strength of cement-based materials. Excessive amounts of crushed gloves create large voids within the mixture, and the poor bonding between SWNGF and cement hydration products results in a decrease in stiffness. Group C exhibits better compressive strength than groups A and B, suggesting that a fiber size of 15 mm × 10 mm is more favorable.

3.1.3 Compressive strain

Figure 5 presents the compressive strain of CG and SWNGF, with detailed data available in Table 3. This section primarily discusses the two types of strain when the specimens reach LOP and MOR. As observed from Figure 5, the compressive strain for all three groups typically increases and then decreases as the SWNGF content rises, with the strains of A-2 and B-2 being greater than that of the CG group. When the fiber content reaches 3%, the compressive strain of all experimental groups is generally smaller than that of the control group. From Table 3, it can be seen that the ε_{LOP} and ε_{MOR} of the CG specimens are 1.55% and 1.77%, respectively. In the groups incorporating waste nitrile gloves fibers, the strain variation range is smaller for group C, while groups A and B show greater variation. Compared to CG, SWNGF shows a slight increase in deformability from ε_{LOP} to ε_{MOR}. This may be due to the fact that SWNGF improves the failure process of the matrix, requiring more deformation from crack initiation to complete failure. The ε_{LOP} and ε_{MOR} of the B-2 group exhibit higher values than those of other groups, reaching 1.66% and 2.40%, respectively. This indicates that a fiber size of 20 mm × 5 mm with a larger aspect ratio is beneficial for compressive strain.

3.1.4 Compressive toughness

Figure 6 depicts the compressive toughness of CG and SWNGF, with corresponding data listed in Table 3. This section primarily discusses five types of toughness when the specimens reach LOP, MOR, T_{d3}, T_{d5}, and T_{d10}. As observed from Figure 6, for SWNGF with waste nitrile gloves fiber sizes A and C, the toughness tends to decrease as the content of waste nitrile gloves fibers increases. However, for SWNGF incorporating fiber size B, the toughness generally shows an increasing trend followed by a decrease as the fiber content increases.

For T_{d3}, T_{d5}, and T_{d10}, C-1 consistently maintains the highest values across all groups, even reaching 0.52 MPa, this suggests that C-1 maintains relatively good level of toughness after failure. Nevertheless, it is observed that both the toughness prior to failure, represented by T_{LOP} and T_{MOR}, and the toughness subsequent to failure, denoted as T_{d3}, T_{d5}, and T_{d10}, exhibit values that are markedly lower than those corresponding to the control group.

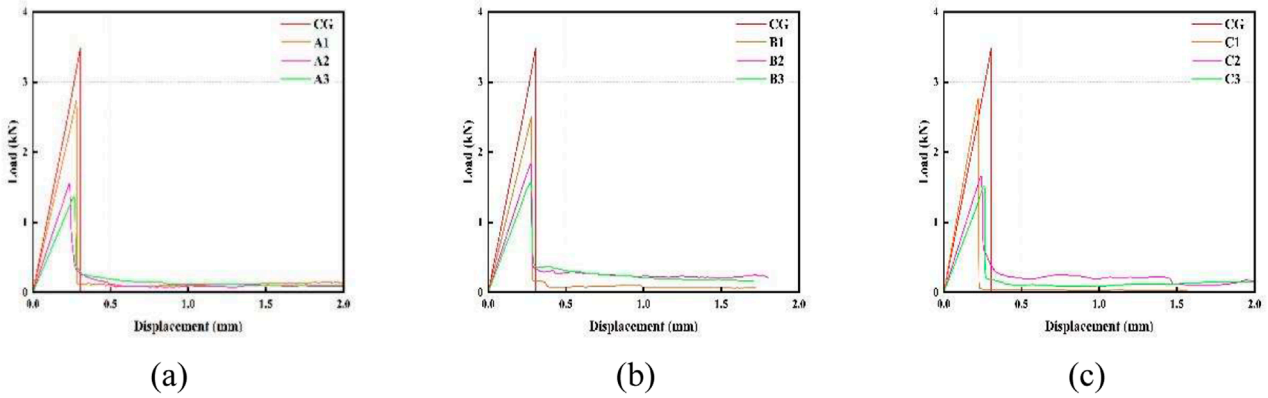

FIGURE 7
Flexural load-deflection curve. **(a)** Group A. **(b)** Group B. **(c)** Group C.

TABLE 4 Flexural performance parameters.

Point	Proformance	Unit	CG	A-1	A-2	A-3	B-1	B-2	B-3	C-1	C-2	C-3
LOP	P_{LOP}	kN	3.95	4.26	1.66	1.44	2.46	1.68	1.31	2.56	1.64	1.58
	f_{LOP}	MPa	9.25	5.58	3.88	3.37	5.77	3.94	3.07	6.01	3.85	3.69
	δ_{LOP}	mm	0.29	0.26	0.26	0.27	0.25	0.29	0.26	0.23	0.26	0.29
	T_{LOP}	N·m	0.56	0.35	0.21	0.20	0.32	0.25	0.17	0.29	0.23	0.23
$d3$	T_{d3}	N·m	0.56	0.40	0.29	0.32	0.35	0.33	0.29	0.33	0.31	0.30
$d5$	T_{d5}	N·m	0.56	0.44	0.35	0.40	0.36	0.35	0.36	0.35	0.35	0.34
$d10$	T_{d10}	N·m	0.56	0.51	0.47	0.55	0.41	0.42	0.52	0.38	0.45	0.43

3.2 Flexural property

3.2.1 Flexural failure process

Figures 7a–c present the load-deflection curves during the flexural process of the specimens for each group. As evidenced by the figures, an increase in the content of broken nitrile glove fibers leads to a gradual reduction in flexural strength. However, with regard to the current Figure 10, the information presented is insufficient to directly deduce the variation trends of toughness and deflection. Following matrix failure, the CG group experiences an immediate loss of load-bearing capacity, whereas in the SWNGF group, the fibers continue to support the load until they are fully pulled out or fractured. Therefore, it can be concluded that, before specimen failure (reaching MOR), SWNGF generally absorbs more energy, and even post-fracture, it continues to dissipate energy. However, with the increase in the content of broken nitrile glove fibers, the amount of energy absorbed decreases. In order to further investigate the flexural mechanical properties, the characteristic parameters derived from the load-deflection curve are presented in detail in Table 4, with each value representing the average of three specimens.

3.2.2 Flexural strength

Figure 8 presents the flexural strength of CG and SWNGF, with detailed data available in Table 4. This section primarily discusses the strength at LOP. Since the control group fractured directly and there was no subsequent phase of increasing load in the load-deflection curves for SWNGF, only the LOP was observed. As shown in Figure 8, the f_{LOP} values for all three groups decreased with the incorporation of waste nitrile glove fibers. In Group A, the f_{LOP} values at 1%, 2%, and 3% fiber content decreased to 5.58 MPa, 3.88 MPa, and 3.37 MPa, respectively. In Group B, the f_{LOP} values at 1%, 2%, and 3% were reduced to 5.77 MPa, 3.94 MPa, and 3.07 MPa, respectively. In Group C, the f_{LOP} values at 1%, 2%, and 3% were 6.01 MPa, 3.85 MPa, and 3.69 MPa, respectively. It can be observed that the 15 mm × 10 mm fiber size seems to be more favorable for flexural strength.

3.2.3 Flexural deflection

Figure 9 shows the flexural deflection of CG and SWNGF, with detailed data available in Table 4. This section primarily discusses the deflection at LOP. As observed from Figure 9, the flexural deflection of Group A remained relatively stable, reaching 0.26 mm, 0.26 mm,

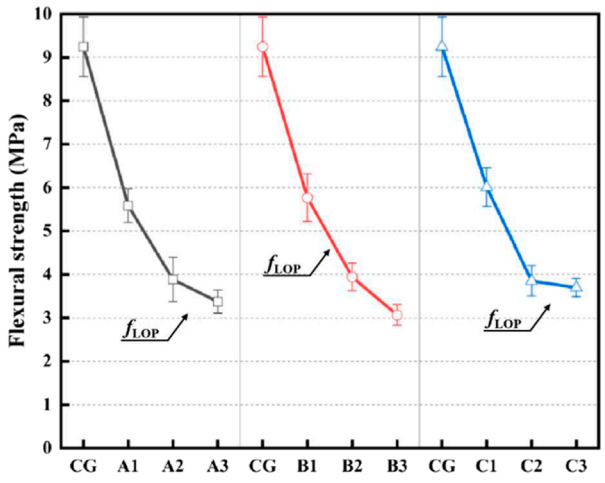

FIGURE 8
Flexural strength of CG and SWNGF.

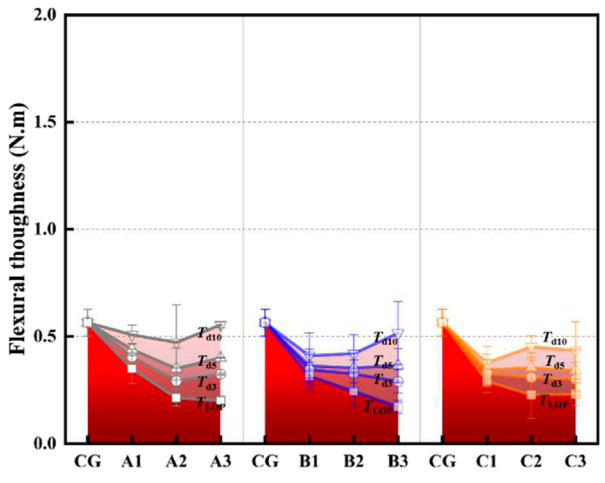

FIGURE 10
Flexural toughness of CG and SWNGF.

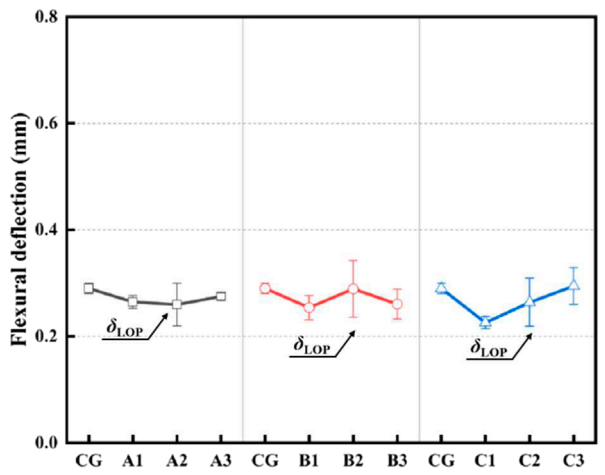

FIGURE 9
Flexural deflection of CG and SWNGF.

and 0.27 mm, respectively. In Group B, the deflection first increased and then decreased, while in Group C, the deflection increased with the increasing content of broken nitrile glove fibers. The maximum δ_{LOP} values for Groups B and C were the same as the control group, both being 0.35 mm. This suggests that the use of fiber sizes A and B has little impact on the flexural deflection of SWNGF. Group C1 exhibited a larger δ_{LOP} (=0.35 mm) than the other groups.

3.2.4 Flexural toughness

Figure 10 presents the flexural toughness of CG and SWNGF, with detailed data available in Table 4. This section focuses on the four types of toughness corresponding to the LOP, *d3*, *d5*, and *d10* values. As observed from Figure 10, the toughness of the specimens increased with the incorporation of broken nitrile glove fibers. The T_{LOP} of the three experimental groups decreased as the fiber content increased. In Group A, the T_{d3}, T_{d5}, and T_{d10} values first decreased and then increased with the increase in fiber content, with T_{d10} reaching nearly the same level as the control group. In Group B, T_{d3} decreased with the increase in fiber content, while T_{d5} and T_{d10} first decreased and then increased. In Group C, both T_{d3} and T_{d5} decreased with increasing fiber content, while T_{d10} exhibited an initial increase followed by a decrease. After specimen failure (reaching LOP), the samples from Group C3 demonstrated significantly better T_{d3}, T_{d5}, and Td10 values. Group C3 showed larger T_{d3} (=0.71 N·m) and T_{d5} (=0.98 N·m) values, while Group A3 exhibited larger T_{d5} (=0.98 N·m) and T_{d10} (=1.63 N·m) values. Overall, although CG exhibited higher flexural strength, it showed an instantaneous failure mode. With the incorporation of broken nitrile gloves, the flexural strength decreased, but the subsequent energy required to maintain the overall integrity of SWNGF increased, providing more time for users to assess the safety of the structure.

3.3 Microscopic material and morphology

Figure 11a presents the SEM image of the broken glove and cement matrix. A well-bonded acrylic glove fragment is clearly visible, with numerous cement particles adhering to the upper surface of the glove fragment, showing a good initial bonding state. The interface transition zone (ITZ) between the glove fragments and the cement matrix has been observed. A gap is visible at the vertical edge of the acrylic glove fragment within the ITZ region. This is the reason for the relatively poor macroscopic performance of SWNGF, as these microcracks may become weak points under loading, potentially leading to crack propagation and failure. However, the flexibility of nitrile rubber allows it to form a cushioning effect within the cement-based material, absorbing and dispersing stress generated by external loads, reducing crack formation and propagation, thereby enhancing strain and toughness.

As shown in Figure 11b, the surface of SWNGF displays an irregular shape, with a rough texture covered by a layer of cement hydration products. The incorporation of SWNGF contributes to the formation of nucleation sites, which creates favorable

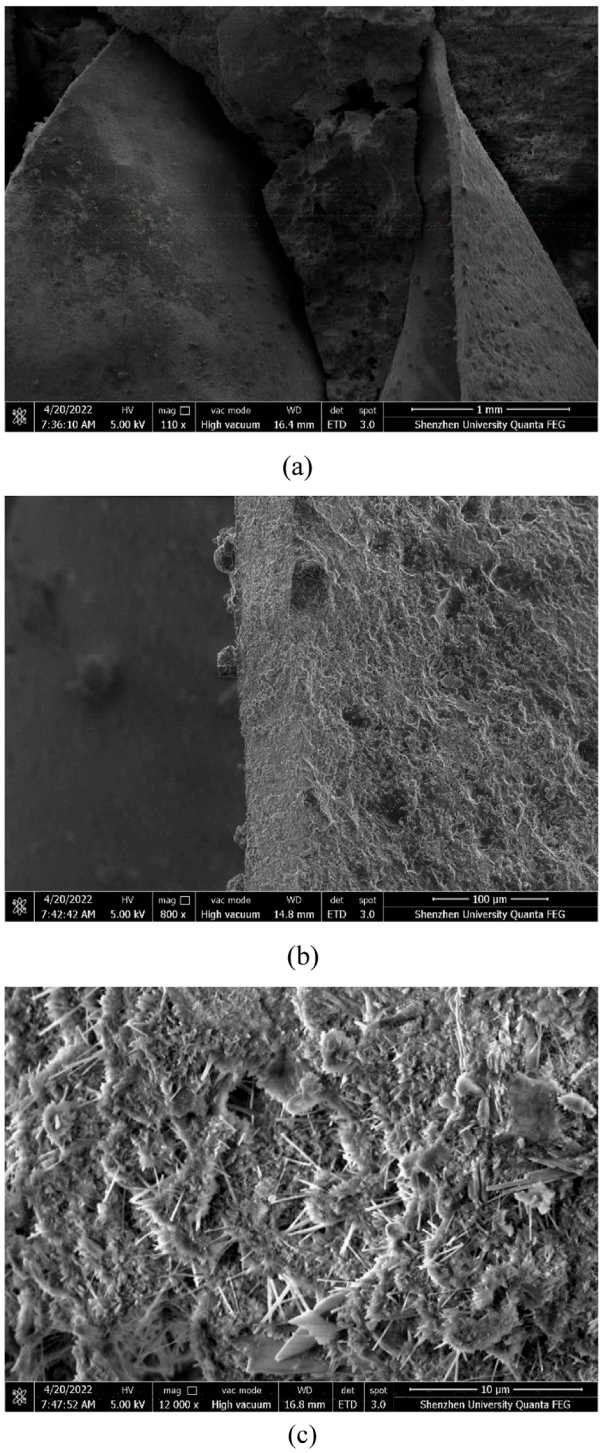

FIGURE 11
Microscopic morphology of fibers and matrix at 28 days of curing age. **(a)** 110×. **(b)** 800×. **(c)** 120,00×.

conditions for the bonding of the cement matrix. This results in improved mechanical and durability properties (He and Lu, 2024a; He et al., 2023; He and Lu, 2024b). A mechanical interlocking structure forms between SWNGF and the cement matrix, thereby improving the bond strength between the two materials.

Figure 11c shows the microstructure of the cement matrix. The crystalline structure of the cement hydration products and the distribution of unhydrated cement particles are clearly visible. Fibrillar C-S-H gel and hexagonal prismatic CH are observed to be forming, while needle-like AFt with rod-like characteristics can also be seen. The C-S-H gel is dense, and the pores vary in shape and size (Liu et al., 2022). Some of the pores are interconnected, which can reduce the compactness and strength of the concrete.

3.4 Environmental impact and application potential

With the frequent occurrence of global public health incidents, the consumption of disposable gloves as an important protective tool has significantly increased. According to statistics, the global monthly consumption of gloves is as high as 65 billion (Prata et al., 2020). These discarded gloves are mainly made of materials such as nitrile rubber, latex, and polyvinyl chloride, which pose a serious threat to the environment and human health due to their non degradability and potential biological and chemical pollution.

The environmental impact of discarded gloves mainly manifests in the following aspects: 1) Glove materials (especially polyvinyl chloride) are difficult to degrade in the natural environment and gradually decompose into microplastic particles. These particles are washed into water bodies by rainwater and eventually merge into the ocean, where they are ingested by marine organisms and accumulated through the food chain, posing potential hazards to ecosystems and human health (Anastopoulos and Pashalidis, 2021); 2) Plasticizers (such as phthalates) and flame retardants in gloves may leach into water and soil, causing environmental pollution. Research has shown that the chemical leaching of PVC gloves in landfills poses a significant threat to groundwater quality (Silva, 2021); 3) Traditional treatment methods such as incineration generate large amounts of harmful gases (such as dioxins, HCl, and SO_2), exacerbating air pollution (Rowan and Laffey, 2021).

Cement can effectively fix hazardous substances in discarded gloves. Research have shown that the complete combustion of one ton of nitrile gloves produces approximately 2.4 tons of CO_2, and that adding 1 ton of waste gloves to concrete can reduce CO_2 emissions by approximately 0.5 tons (Purnomo et al., 2021), and the release of microplastics is reduced by 90% compared to landfilling. The application of discarded gloves in concrete has been validated by some research. Kilmartin-Lynch et al. (2022) added a small amount (<0.3%) of disposable nitrile gloves to concrete, which increased the compressive strength by about 20%. Mousavi and Dehestani (2022), Mousavi and Dehestani (2023) found that using vinyl waste gloves for producing recycled fibers can be used for 3D printing concrete. Ran et al. (2023) found that the compressive strength of rubber glove fibers improved the fatigue resistance of concrete, and discussed the disinfection method of personal protective equipment. The most convenient method is to store it in a specific location for a period of time, and the virus is only active on the surface of the object for a period of time (such as 72 h for plastic).

4 Conclusion

This study aims to explore the effective application of waste nitrile gloves in cement-based materials. Through a series of experimental analyses, it examines their impact on the mechanical properties of cement-based materials, providing a reference for the application of waste nitrile glove concrete in engineering practices.

1) The compressive strength of SWNGF decreases with increasing incorporation of waste nitrile glove fibers, indicating that higher fiber content is detrimental to compressive strength. Among the tested specimens, those with a fiber size of 15 mm × 10 mm exhibit relatively better compressive strength. The compressive strain of the three groups initially increases and then decreases as the SWNGF content increases. The strain of groups A-2 and B-2 is greater than that of the control group, and fibers with a size of 20 mm × 5 mm are beneficial for compressive strain. Group C-1 demonstrates better toughness after failure, but its overall performance remains lower than that of the control group.
2) After the incorporation of waste nitrile glove fibers, the flexural strength of SWNGF decreases in all three groups of specimens, with a fiber size of 15 mm × 10 mm being relatively advantageous for flexural strength. The sizes A and B have little effect on the flexural modulus of SWNGF, while group C1 shows the maximum deflection. SWNGF exhibits improved toughness after failure, which increases with the content of SWNGF, with group A3 showing better performance in T_{d5} and T_{d10}.
3) The surface of SWNGF is irregular and covered with cement hydration products, forming a mechanical interlocking structure with the cement matrix that enhances the bond strength. Gaps exist between the broken gloves and the cement matrix, which is the reason for the relatively poor macroscopic performance of SWNGF. However, the flexibility of nitrile rubber creates a cushioning effect, absorbing and dispersing stress, thereby increasing strain and toughness.

In summary, the incorporation of waste nitrile glove fibers has a multifaceted impact on the mechanical properties of cement-based materials. In engineering applications, it is essential to comprehensively consider their effects on strength, deformability, and energy absorption capacity. The fiber content and size should be carefully selected to optimize both the utilization of waste resources and the performance of the concrete.

Data availability statement

The original contributions presented in the study are included in the article/supplementary material, further inquiries can be directed to the corresponding author.

Author contributions

HT: Conceptualization, Data curation, Formal Analysis, Visualization, Writing – original draft. BF: Investigation, Methodology, Software, Writing – original draft. YL: Investigation, Validation, Writing – original draft. JZ: Validation, Writing – original draft. JL: Formal Analysis, Validation, Writing – original draft. JL: Funding acquisition, Methodology, Writing – review and editing. SY: Data curation, Formal Analysis, Resources, Supervision, Writing – review and editing.

Funding

The author(s) declare that financial support was received for the research and/or publication of this article. The work described in this paper was fully supported by grants Shenzhen Science and Technology Program (KCXFZ20230731092804009) and Guangdong Provincial Key Laboratory of Durability for Marine Civil Engineering (SZU) (2020B1212060074).

Conflict of interest

Authors HT and BF were employed by CCCC-SHEC Dongmeng Engineering Co., Ltd.

The remaining authors declare that the research was conducted in the absence of any commercial or financial relationships that could be construed as a potential conflict of interest.

Generative AI statement

The authors declare that no Generative AI was used in the creation of this manuscript.

Publisher's note

References

Anastopoulos, I., and Pashalidis, I. (2021). Single-use surgical face masks, as a potential source of microplastics: do they act as pollutant carriers? *J. Mol. Liq.* 326, 115247. doi:10.1016/j.molliq.2020.115247

Asim, N., Badiei, M., and Sopian, K. (2021). Review of the valorization options for the proper disposal of face masks during the COVID-19 pandemic. *Environ. Technol. Innov.* 23, 101797. doi:10.1016/j.eti.2021.101797

ASTM C 1018-97 (1998). *Structural test method for flexural toughness and first crack strength of fiber reinforced concrete (using beam with third point loading)*. American Society of Testing and Materials, 514–551.

Boroujeni, M., Saberian, M., and Li, J. (2021). Environmental impacts of COVID-19 on Victoria, Australia, witnessed two waves of Coronavirus. *Environ. Sci. Pollut. Res.* 28, 14182–14191. doi:10.1007/s11356-021-12556-y

Cao, C., Xie, Y., Liu, Y., Liu, J., and Zhang, F. (2023a). Two-phase COVID-19 medical waste transport optimisation considering sustainability and infection probability. *J. Clean. Prod.* 389, 135985. doi:10.1016/j.jclepro.2023.135985

Cao, C., Liu, J., Liu, Y., Wang, H., and Liu, M. (2023b). Digital twin-driven robust bi-level optimisation model for COVID-19 medical waste location-transport under circular economy. *Comput. Ind. Eng.* 186, 109107. doi:10.1016/j.cie.2023.109107

Cheng, L., Jin, H., Zhang, W., Xie, G., Liu, J., and Xing, F. (2024). Influence of municipal solid waste incineration bottom ash on the hydration and carbonation behavior of reactive magnesia cement. *Chem. Eng. J.* 502, 158059. doi:10.1016/j.cej.2024.158059

Chowdhury, T., Chowdhury, H., Rahman, M. S., Hossain, N., Ahmed, A., and Sait, S. M. (2022). Estimation of the healthcare waste generation during COVID-19 pandemic in Bangladesh. *Sci. Total Environ.* 811, 152295. doi:10.1016/j.scitotenv.2021.152295

Chua, M. H., Cheng, W., Goh, S. S., Kong, J., Li, B., Lim, J. Y. C., et al. (2020). Face masks in the new COVID-19 Normal: materials, testing, and perspectives. *Research (Wash. DC)* 2020, 7286735. doi:10.34133/2020/7286735

Dadwal, T., Kumar, V., and Bhatia, U. (2023). Experimental investigation on the use of COVID-19 waste in bituminous concrete. *Mater. Today Proc.* 74, 218–224. doi:10.1016/j.matpr.2022.08.055

Demir, A. T., and Moslem, S. (2024). Evaluating the effect of the COVID-19 pandemic on medical waste disposal using preference selection index with CRADIS in a fuzzy environment. *Heliyon* 10, e26997. doi:10.1016/j.heliyon.2024.e26997

GB 175 (2023). *General purpose Portland cement*. Beijing, China: Chinese National Standard.

GB/T 17671. (1999). *Method of testing cements-Determination of strength (ISO Method)*.

He, R., and Lu, N. (2024a). Hydration, fresh, mechanical, and freeze-thaw properties of cement mortar incorporated with polymeric microspheres. *Adv. Compos. Hybrid. Mater.* 7, 92. doi:10.1007/s42114-024-00899-2

He, R., and Lu, N. (2024b). Air void system and freezing-thawing resistance of concrete composite with the incorporation of thermo-expansive polymeric microspheres. *Constr. Build. Mater.* 419, 135535. doi:10.1016/j.conbuildmat.2024.135535

He, R., Nantung, T., Olek, J., and Lu, N. (2023). Field study of the dielectric constant of concrete: a parameter less sensitive to environmental variations than electrical resistivity. *J. Build. Eng.* 74, 106938. doi:10.1016/j.jobe.2023.106938

Idowu, G. A., and Olonimoyo, E. A. (2023). How has COVID-19 medical face mask altered the dynamics of pollutants from incinerated wastes? *J. Hazard. Mater. Adv.* 11, 100351. doi:10.1016/j.hazadv.2023.100351

JGJ 63-2006 (2006). *Standard of water for concrete*. Beijing, China: Chinese National Standard.

Karimi, H., Wassan, N., Ehsani, B., Tavakkoli-Moghaddam, R., and Ghodratnama, A. (2024). Optimizing COVID-19 medical waste management using goal and robust possibilistic programming. *Eng. Appl. Artif. Intell.* 131, 107838. doi:10.1016/j.engappai.2023.107838

Kilmartin-Lynch, S., Roychand, R., Saberian, M., Li, J., and Zhang, G. (2022). Application of COVID-19 single-use shredded nitrile gloves in structural concrete: case study from Australia. *Sci. Total Environ.* 812, 151423. doi:10.1016/j.scitotenv.2021.151423

Liu, J., Zhang, W., Li, Z., Jin, H., and Tang, L. (2022). Mechanics, hydration phase and pore development of embodied energy and carbon composites based on ultrahigh-volume low-carbon cement with limestone calcined clay. *Case Stud. Constr. Mater.* 17, e01299. doi:10.1016/j.cscm.2022.e01299

Masud, R. I., Suman, K. H., Tasnim, S., Begum, M. S., Sikder, M. H., Uddin, M. J., et al. (2023). A review on enhanced microplastics derived from biomedical waste during the COVID-19 pandemic with its toxicity, health risks, and biomarkers. *Environ. Res.* 216, 114434. doi:10.1016/j.envres.2022.114434

MDS (2023). *A Glove's Biodegradation process in Anaerobic landfill*. Eco-MDS Associates. Available online at: https://eco-mdsassociates.com/blogs/news/biodegradable-nitrile-glove-briefing.

Mousavi, S. S., and Dehestani, M. (2022). Influence of latex and vinyl disposable gloves as recycled fibers in 3D printing sustainable mortars. *Sustainability* 14, 9908. doi:10.3390/su14169908

Mousavi, S. S., and Dehestani, M. (2023). On the possibility of using waste disposable gloves as recycled fibers in sustainable 3D concrete printing using different additives. *Sci. Rep.* 13, 10812. doi:10.1038/s41598-023-37803-9

Park, S. (2023). Assessing the impact of COVID-19 on waste generation: focus on plastic, food, and medical wastes in South Korea. *Heliyon* 9, e18881. doi:10.1016/j.heliyon.2023.e18881

Patrawoot, S., Tran, T., Arunchaiya, M., Somsongkul, V., Chisti, Y., and Hansupalak, N. (2021). Environmental impacts of examination gloves made of natural rubber and nitrile rubber, identified by life-cycle assessment. *SPE Polym.* 2, 179–190. doi:10.1002/pls2.10036

Prata, J. C., Silva, A. L. P., Walker, T. R., Duarte, A. C., and Rocha-Santos, T. (2020). COVID-19 pandemic repercussions on the use and management of plastics. *Environ. Sci. Technol.* 54, 7760–7765. doi:10.1021/acs.est.0c02178

Purnomo, C. W., Kurniawan, W., and Aziz, M. (2021). Technological review on thermochemical conversion of COVID-19-related medical wastes. *Resour. Conserv. Recycl.* 167, 105429. doi:10.1016/j.resconrec.2021.105429

Ramalingam, S., Thamizhvel, R., Sudagar, S., and Silambarasan, R. (2023). Production of third generation bio-fuel through thermal cracking process by utilizing Covid-19 plastic wastes. *Mater. Today Proc.* 72, 1618–1623. doi:10.1016/j.matpr.2022.09.430

Ran, T., Pang, J., and Zou, J. (2022). An emerging solution for medical waste: reuse of COVID-19 protective suit in concrete. *Sustainability* 14, 10045. doi:10.3390/su141610045

Ran, T., Pang, J., Liu, Y., Zou, J., and Cai, F. (2023). Improving concrete fatigue resistance with COVID-19 rubber gloves: an innovative sustainable approach. *Case Stud. Constr. Mater.* 18, e01914. doi:10.1016/j.cscm.2023.e01914

Rowan, N. J., and Laffey, J. G. (2021). Unlocking the surge in demand for personal and protective equipment (PPE) and improvised face coverings arising from coronavirus disease (COVID-19) pandemic – implications for efficacy, re-use and sustainable waste management. *Sci. Total Environ.* 752, 142259. doi:10.1016/j.scitotenv.2020.142259

Saberian, M., Li, J., Kilmartin-Lynch, S., and Boroujeni, M. (2021). Repurposing of COVID-19 single-use face masks for pavements base/subbase. *Sci. Total Environ.* 769, 145527. doi:10.1016/j.scitotenv.2021.145527

Sangkham, S. (2020). Face mask and medical waste disposal during the novel COVID-19 pandemic in Asia. *Case Stud. Chem. Environ. Eng.* 2, 100052. doi:10.1016/j.cscee.2020.100052

Silva, A. L. P. (2021). Increased plastic pollution due to COVID-19 pandemic Challenges and recommendations. *Chem. Eng.* doi:10.1016/j.cej.2020.126683

Tang, J., Liu, X., and Wang, W. (2023). COVID-19 medical waste transportation risk evaluation integrating type-2 fuzzy total interpretive structural modeling and Bayesian network. *Expert Syst. Appl.* 213, 118885. doi:10.1016/j.eswa.2022.118885

Telugunta, R., Choudhary, S., and Sumant, O. (2021). "Gloves market by type (disposable sterile gloves, disposable examination and protective gloves, and consumer gloves), and industry (medical, horeca (food), cleaning, beauty, food and drinks, pharmaceutical, chemical, automotive, electronics, construction, and others)," in *Global opportunity analysis and industry forecast 2021–2025*.

Zeng, F., Liu, D., Xiao, C., Li, K., Qian, X., He, Y., et al. (2024). Advances and perspectives on the life-cycle impact assessment of personal protective equipment in the post-COVID-19 pandemic. *J. Clean. Prod.* 437, 140783. doi:10.1016/j.jclepro.2024.140783

Zhang, W., Zheng, C., Li, Z., Jin, H., Liu, J., Zhu, J., et al. (2022). Investigation on mechanical properties improvement of seawater engineered cementitious composites (ECC) using FA/LC2. *Constr. Build. Mater.* 345, 128271. doi:10.1016/j.conbuildmat.2022.128271

Zhu, J., Saberian, M., Anupiya, S. T., Perera, M., Roychand, R., Li, J., et al. (2022). Reusing COVID-19 disposable nitrile gloves to improve the mechanical properties of expansive clay subgrade: an innovative medical waste solution. *J. Clean. Prod.* 375, 134086. doi:10.1016/j.jclepro.2022.134086